IEEE Photonics Journal
An IEEE Photonics Society Publication

A Discrete Model for Resonance Near Embedded Bound States

Volume 2, Number 6, December 2010

Stephen P. Shipman
Jennifer Ribbeck
Katherine H. Smith
Clayton Weeks

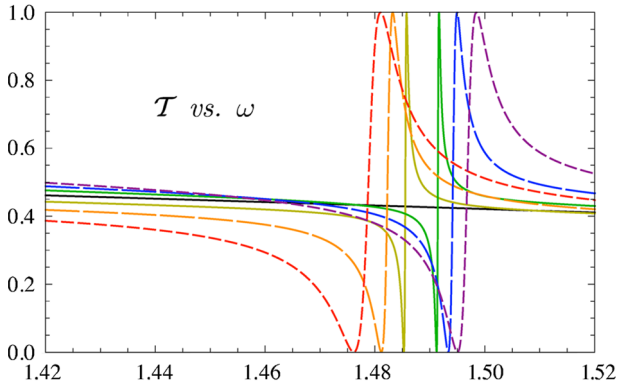

DOI: 10.1109/JPHOT.2010.2080314
1943-0655/$26.00 ©2010 IEEE

IEEE photonics SOCIETY
IEEE

A Discrete Model for Resonance Near Embedded Bound States

Stephen P. Shipman, Jennifer Ribbeck, Katherine H. Smith, and Clayton Weeks

Department of Mathematics, Louisiana State University, Baton Rouge, LA 70803 USA

DOI: 10.1109/JPHOT.2010.2080314
1943-0655/$26.00 ©2010 IEEE

Manuscript received August 14, 2010; revised September 17, 2010; accepted September 17, 2010. Date of publication September 23, 2010; date of current version Month 00, 0000. This work was supported by the National Science Foundation (NSF) under Grant DMS-0807325 (S. P. Shipman), by NSF VIGRE Grant DMS-0739382 (J. Ribbeck, K. H. Smith, and C. Weeks), and by a Louisiana State University CFLR scholarship (K. H. Smith). Corresponding author: S. P. Shipman (e-mail: shipman@math.lsu.edu).

Abstract: We present a discrete model for resonance in periodic dielectric slabs arising from the interaction of electromagnetic plane waves with guided modes at frequencies embedded in the continuum. Two infinite rows of interacting masses in the model support propagating and evanescent waves simultaneously. This allows for modes to be exponentially trapped near an obstacle at continuum frequencies. The discrete model manifests resonant transmission features of the periodic slab, and it includes parameters of asymmetry that are connected to the detuning of the resonance. Moreover, resonant transmission in both systems is described by a rigorous universal formula that explicitly incorporates a detuning parameter.

Index Terms: Guided mode, modeling, scattering, theory, transmission resonance.

1. Introduction

When electromagnetic plane waves in air are scattered by a periodic slab, resonant interaction with guided modes of the slab is known to cause anomalies in the scattered field, which are manifest as sharp peaks and dips in the transmission versus frequency graph near the guided mode frequency [1]–[3], e.g., the tuning of sharp transmission features is important for photo-electronic devices and has been examined in discrete [4], [5] and continuous [4], [6], [7] models, using a variety of resonators, defects, and impurities.

Two salient features of a resonance are its central frequency and its width, and the tuning of both is important in applications such as PC light-emitting-diodes [6]. The width is often associated with how far the system is perturbed from an ideal one that supports a guided mode (a bound state). The center of a resonance is primarily determined by the frequency of the mode, but it can be detuned significantly by small perturbations of the system. In fact, the detuning of a resonance is connected with structural asymmetry [8], [9], and this idea will be highlighted in this article. By choosing suitable perturbation parameters, one seeks to control the center and width of a resonance.

The purpose of this work is to provide a simple discrete model (see Fig. 1) for plane-wave/guided-mode resonant interaction for lossless periodic slabs. Its main features are the following.

1) It possesses a key feature of the air/slab system that is not present in the Anderson discrete model [10]: An exponentially localized embedded bound state is supported by the physically coupled system. This feature is achieved by using two infinite chains of beads that simultaneously support both a propagating and an evanescent field in the same frequency interval.

2) The model explicitly incorporates two parameters of asymmetry, one in the chains of beads (modeling the ambient space) and one in the scatterer, which consists of two beads whose masses differ from those of the rest of the beads in the chains. We will show how these two parameters affect the center and width of a transmission resonance.
3) The model is complex enough to capture the essential features of slab anomalies but simple enough to admit exact calculations by hand. This facilitates the analytical investigation of the correspondence between parameters of the transmission resonance and those of the structure.
4) The transmission resonances of the air/slab system and the discrete system are unified through a rigorous formula that we derived in [8] and [11], which is discussed in Section 3.

The crucial characteristic of the kind of bound state that we are considering is that it is *nonrobust*. By this we mean that it is supported by a system whose parameters (geometrical, material, angle of incidence, etc.) are tuned to specific values that inhibit the coupling between the bound state and the extended states of the continuum. Under a generic perturbation of these parameters, coupling to the continuum destroys the bound state. In the case of a periodic dielectric slab in contact with the surrounding air, symmetry of the structure about a plane perpendicular to the slab suppresses the propagating diffractive order of anti-symmetric fields, thus creating a guided mode exponentially bound to slab at a frequency embedded in the continuous spectrum (spectral band) of the slab/air system. A perturbation of the wave vector or structure initiates a coupling to the propagating harmonic, thus destroying the mode and creating transmission resonance [11]. It is this type of nonrobust bound state that our discrete system models.

The nonleaky nature of these special guided modes is discussed in [12] (see Figs. 5 and 6), and an enlightening exposition of these modes as well as leaky modes, whose radiation losses are due to the interaction with plane waves, is given in [13, Sec. 2.2] (see Fig. 3). In [3] (see Fig. 4), the authors discuss the practical utility of a sharp transmission resonance that emerges when the symmetry of a structure that supports a guided mode is broken.

Of evident practical and theoretical importance is the obtention of analytic formulas for transmission anomalies with tunable parameters. Fano's formula [14], which is discussed below, is based on the interaction between a continuum of extended states with an embedded bound state and is characterized by a single peak and dip. This type of resonance is commonly referred to as Fano resonance. The need to refine this formula for applications in photonics has led to various analytic models. Fan and Joannopoulos [2] develop a model based on the principle of interference between a direct pathway of transmission and an indirect resonant one. A more general temporal coupled-mode theory developed in [15] is able to capture fine quantitative features of a variety of photonic resonances [3], [16], [17]. Other coupled-mode theories, such as [18], are specific to plasmon-enhanced transmission. In the last few years, great progress in electric circuit models has rendered them a powerful tool for the quantitative description of resonant transmission (see [19]–[22] and references therein).

In this paper (see Section 3), we show how transmission anomalies of both a lossless periodic dielectric air/slab system as well as our discrete model are described by a rigorous analytic formula derived in [8] and [11]. It is based on the principle of nonrobustness of a (nonleaky) bound state with respect to structural parameters or the Bloch wave vector κ parallel to the slab and the analytic perturbation of an associated operator equation with respect to these parameters. The formula is attractive for several reasons: It is rigorous, that is, it follows mathematically from the resonant system itself (continuous or discrete) and not from analysis based on phenomenological principles; the peak, dip, and detuning are represented in an explicit way; it can be refined to arbitrary order of accuracy; and it is based on very general arguments, making it applicable to scattering by continuous and discrete systems for which reflection and transmission coefficients are defined and that possesses a nonrobust embedded bound mode. Thus, we have the assurance that our discrete model faithfully captures the resonant features of the continuous one. It incorporates, in an intuitive and transparent way, parameters that track the movement of the peak and dip—and, therefore, the center and width of the resonance as well—as the system is perturbed. It subsumes the formula of

Fano [see (1) shown below] under conditions that can be characterized in terms of salient features of the frequency versus transmission graph.

Let us briefly review the models of Fano and Anderson and compare their features to those of a resonant periodic slab system and our discrete model.

In the Fano and Anderson models, one begins with two physical systems decoupled from one another. One system is an infinite string (continuous or discrete) and thus possesses a continuous spectral band, while the other, which is a harmonic resonator, possesses a single characteristic frequency. The frequency ω_0 of the oscillator is taken to lie in the spectral band of the string so that the decoupled ensemble of both systems has ω_0 as an eigenvalue embedded in its continuous spectrum, with bound (finite-energy) eigenstate corresponding to the oscillation of the resonator. When one couples the resonator to the string, the eigenvalue dissolves into the continuous spectrum as the bound state ceases to exist. The resulting alteration of the extended states of the string is pronounced near ω_0, leading to a sharp anomaly in the transmission coefficient for the coupled system. The anomaly typically has a peak and a dip for which Fano [14] derived the approximate shape

$$f_q(e) = \text{const.}\frac{|q+e|^2}{1+e^2}, \qquad e = \frac{E-E_{\text{res}}}{\Gamma/2} \tag{1}$$

where e represents the energy normalized to a characteristic width Γ of the anomaly.

In the problem of scattering by a periodic dielectric slab, the role of a bound state is played by a guided mode. The slab is never physically decoupled from the ambient air, and therefore, the oscillations of any guided mode extend evanescently into the surrounding medium. It is this latter feature that distinguishes our discrete model from the Anderson model: We present a physically coupled system that supports states that are exponentially confined near the scatterer. Note that a one-chain Anderson model in which a resonator is coupled to multiple lattice points can support embedded bound states [23]. However, these states do not extend evanescently into the infinite chain; moreover, we need more than one chain for the modeling of asymmetry.

2. Discrete Model

The transmission anomaly of the slab system, as we have discussed, relies crucially on the fact that the slab supports a guided mode at an *isolated* real wavenumber-frequency pair (κ_0, ω_0), where ω_0 is embedded in the continuum (κ_0 being in the plane of the slab). Such a nonrobust mode is sustained even though the slab is in physical contact with the ambient space; this is possible because of the presence of both propagating and evanescent spatial harmonics.

In a discrete model in which the ambient space is modeled by coupled beads, two harmonics can be achieved minimally with two infinite rows of beads, and within a suitable frequency range, one of the harmonics will be propagating and the other evanescent. Our model is illustrated in Fig. 1. It consists of two parallel infinite rows of masses connected by taut strings to each other and to two fixed parallel anchors. The masses are constrained to move only in the out-of-plane direction. The rows are indexed by $n = 0, 1$, whereas the beads in each row are indexed by $m = -\infty, \ldots, \infty$. All beads have the same mass 1 except for the two at $m = 0$, which act as a scatterer of waves in the ambient lattice. For a symmetric system, the tensions in all strings are taken to be 1 and the masses at $m = 0$ are taken to be equal to each other. Asymmetry in the ambient lattice is imposed by perturbing the tensions of the strings attached to the anchors for $m \neq 0$ by η at the top and by $-\eta$ at the bottom. Asymmetry in the scatterer is imposed by making the masses at $m = 0$, which we call M_0 and M_1, unequal.

The lattice is subject to linear Newtonian dynamics, in which the force at any site is the sum of the relative displacements of each of its nearest neighbors multiplied by the corresponding tensions of the connecting strings. If the displacements of the beads are denoted by $U = \{U_{mn}\}$, their velocities by $\dot{U} = \{\dot{U}_{mn}\}$, and their momenta by $P = \{P_{mn} = M_{mn}\dot{U}_{mn}\}$, the Hamiltonian is

$$H(U,P) = \sum_{m=-\infty}^{\infty}\sum_{n=0}^{1}\left[\frac{1}{2M_{mn}}P_{mn}^2 + +\frac{1}{2}(\tau_{mn}+3)U_{mn}^2 - U_{mn}(U_{m+1,n}+U_{m-1,n}+U_{mn})\right] \tag{2}$$

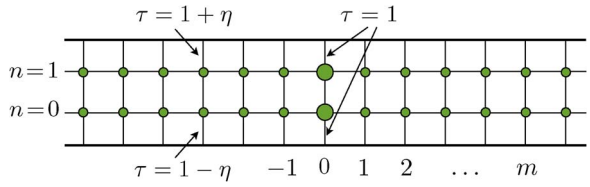

Fig. 1. Lattice model for resonant interaction between extended states and trapped modes at frequencies embedded in the continuum. The scatterer that supports the trapped modes consists of the two beads at $m = 0$ whose masses (which are denoted by M_0 and M_1) differ from those of rest of the lattice. Asymmetry in the lattice is imposed by changing the upper and lower tensions by $\pm\eta$ for $m \neq 0$, and asymmetry in the scatterer is imposed by taking $M_0 \neq M_1$.

in which $\tau_{mn} = 1$ if $m = 0$, $\tau_{mn} = 1 - (-1)^n\eta$ if $m \neq 0$, and $\hat{n} = 1 - n$ for $n = 0, 1$. This results in the system of ordinary differential equations

$$M_n\ddot{U}_{0n} = -4U_{0n} + U_{1n} + U_{-1n} + U_{0\hat{n}} \tag{3}$$

$$\ddot{U}_{mn} = \big((-1)^n\eta - 4\big)U_{mn} + U_{m+1,n} + U_{m-1,n} + U_{m\hat{n}}, \quad \text{for } m \neq 0. \tag{4}$$

The assumption of a harmonic solution $U_{mn}(t) = u_{mn}e^{-i\omega t}$ with $\omega > 0$ leads to the equations

$$(M_n\omega^2 - 4)u_{0n} + u_{1n} + u_{-1n} + u_{0\hat{n}} = 0 \tag{5}$$

$$\big(\omega^2 + (-1)^n\eta - 4\big)u_{mn} + u_{m+1,n} + u_{m-1,n} + u_{m\hat{n}} = 0, \quad \text{for } m \neq 0. \tag{6}$$

The table below identifies the correspondence of parameters and physical objects between the slab system and the discrete model.

dielectric slab system	discrete model
ambient space (air)	uniform lattice at $m \neq 0$
periodic slab (scatterer of plane waves)	the scatterer : anomalous masses M_0 and M_1 at $m = 0$
frequency ω	frequency ω
wave number κ parallel to the slab (equivalently, angle of incidence)	tension of the strings in the ambient lattice ($\tau = 1 \pm \eta$)
structural symmetry about a plane perpendicular to the slab	equal masses of the scatterer ($M_0 = M_1$)
Maxwell system or the wave equation	ODE system (3, 4)
harmonic Maxwell system or Helmholtz equation	equations (5, 6)
propagating diffraction orders	solutions $q_n e^{\pm i\theta m}$ in the uniform lattice
evanescent diffraction orders	solutions $q_n e^{-\alpha\lvert m\rvert}$, α>0, in the uniform lattice
bound state : a guided mode exponentially confined to the slab	bound state : a trapped mode exponentially confined to the scatterer

The uniform lattice. Because the uniform ambient lattice consists of two rows of beads, the general solution for $m \neq 0$ is a combination of two separable solutions of the form

$$u_{mn} = q_n h_m.$$

Assuming the form $h_m = r^m$, we obtain

$$r^2 + \left[\big(\omega^2 - 4 + (-1)^n\eta\big) + \frac{q_{\hat{n}}}{q_n}\right] r + 1 = 0 \tag{7}$$

for $n = 0, 1$. We must find ratios q_0/q_1 and numbers r that satisfy this equation for both $n = 0$ and $n = 1$. Thus, we require

$$(\omega^2 - 4 + \eta) + \frac{q_1}{q_0} = (\omega^2 - 4 - \eta) + \frac{q_0}{q_1}$$

which yields either

$$\frac{q_0}{q_1} = \frac{q_0^{\mathrm{p}}}{q_1^{\mathrm{p}}} = \eta + \sqrt{1+\eta^2} \quad \text{or} \quad \frac{q_0}{q_1} = \frac{q_0^{\mathrm{e}}}{q_1^{\mathrm{e}}} = \eta - \sqrt{1+\eta^2}$$

where the superscripts p and e are used in anticipation of the propagating and evanescent nature of the harmonics for the particular frequency interval that we will choose to work with (9), shown below.

Using these ratios in (7), we find that r satisfies

$$r^2 - br + 1 = 0 \tag{8}$$

where b is one of the two numbers

$$b^{\mathrm{p}} = 4 - \omega^2 - \sqrt{1+\eta^2}, \qquad b^{\mathrm{e}} = 4 - \omega^2 + \sqrt{1+\eta^2}.$$

The solutions of (8) are reciprocal to each other, that is, they are equal to $(r^{\mathrm{p}})^{\pm 1}$ or $(r^{\mathrm{e}})^{\pm 1}$, where

$$r^{\mathrm{p}} = \frac{1}{2}\left[b^{\mathrm{p}} + \sqrt{(b^{\mathrm{p}})^2 - 4}\right], \qquad r^{\mathrm{e}} = \frac{1}{2}\left[b^{\mathrm{e}} + \sqrt{(b^{\mathrm{e}})^2 - 4}\right].$$

One finds that, as long as the inequalities

$$-\sqrt{1-\eta^2} < \omega^2 - 2 < \sqrt{1-\eta^2} \tag{9}$$

hold, r^{p} has unit modulus, and r^{e} is real and greater than 1. We can thus define $0 < \theta < \pi$ and $\alpha > 0$ so that

$$r^{\mathrm{p}} = e^{i\theta}, \quad r^{\mathrm{e}} = e^{\alpha}. \tag{10}$$

The general solution of (6) in the uniform lattice (all masses equal to 1) is a combination of separable solutions

$$u_{mn} = q_n^{\mathrm{p}}\left(c_1^{\mathrm{p}} e^{i\theta m} + c_2^{\mathrm{p}} e^{-i\theta m}\right) + q_n^{\mathrm{e}}\left(c_1^{\mathrm{e}} e^{\alpha m} + c_2^{\mathrm{e}} e^{-\alpha m}\right). \tag{11}$$

When multiplied by $e^{-i\omega t}$, the first two terms represent waves traveling to the right and left, and the last two represent exponentially growing and decaying solutions.

In the symmetric case $\eta = 0$, the ratios

$$q_0^{\mathrm{p}}/q_1^{\mathrm{p}} = 1, \qquad q_0^{\mathrm{e}}/q_1^{\mathrm{e}} = -1$$

indicate that, in a propagating harmonic, the two rows of beads are displaced by identical amounts, whereas in an evanescent harmonic, the two rows are displaced by the same magnitude but in opposite directions.

The entire continuous spectrum (spectral band) for the uniform lattice system consists of those frequencies for which at least one of the two values of r in (8) is unitary (a complex number with unit modulus). For $\eta = 0$, for example, one of the values of r is unitary when $1 \le \omega^2 \le 5$, and the other is unitary when $3 \le \omega^2 \le 7$, and thus, the spectral band is $1 \le \omega^2 \le 7$. The angle of the values of r is graphed in Fig. 2; this is the dispersion relation for the uniform lattice. It is bivalued in the interval $3 \le \omega^2 \le 5$, and there are two intervals, i.e., $1 \le \omega^2 < 3$ and $5 < \omega^2 \le 7$, for which there is exactly one propagating harmonic. The interval (9) for $\eta = 0$ is precisely $1 < \omega^2 < 3$.

Scattering. When an obstacle is introduced into the lattice by the modification of the masses at $m = 0$, a right-traveling wave $I^{\mathrm{p}} q_n^{\mathrm{p}} e^{i\theta m}$ of amplitude $|I^{\mathrm{p}}|$ is scattered by the obstacle, producing a

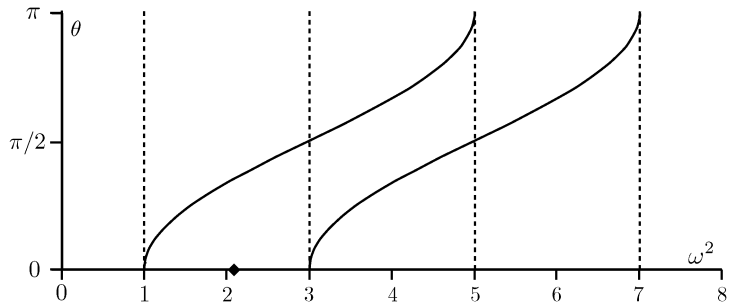

Fig. 2. Dispersion relation for the uniform lattice when $\eta = 0$. The graphs of $\theta = \arccos((3-\omega^2)/2)$ and $\theta = \arccos((5-\omega^2)/2)$ give θ in the propagating harmonic $q_n e^{\pm i\theta m}$ as a function of ω^2. The spectral band is the interval $1 \le \omega^2 \le 7$, in which there exists at least one such value of θ. In the intervals $1 \le \omega^2 < 3$ and $5 < \omega^2 \le 7$, there is exactly one propagating harmonic, and therefore, it is possible that the system with the scatterer, for suitable values of M_0 and M_1, support a trapped mode built only from the evanescent harmonic that decays exponentially as $|m| \to \infty$. When $(M_0, M_1) = (2, 2)$ and $\eta = 0$, such a mode exists at $\omega^2 = 21/10$, as indicated by the diamond. This frequency is embedded in the continuous spectrum.

reflected wave $A^{\mathrm{p}} q_n^{\mathrm{p}} e^{-i\theta m}$ to the left and a transmitted wave $B^{\mathrm{p}} q_n^{\mathrm{p}} e^{i\theta m}$ to the right. In addition, evanescent harmonics emerge in the vicinity of the obstacle

$$u_{mn} = \begin{cases} I^{\mathrm{p}} q_n^{\mathrm{p}} e^{i\theta m} + A^{\mathrm{p}} q_n^{\mathrm{p}} e^{-i\theta m} + A^{\mathrm{e}} q_n^{\mathrm{e}} e^{\alpha m}, & m \le 0, \\ B^{\mathrm{p}} q_n^{\mathrm{p}} e^{i\theta m} + B^{\mathrm{e}} q_n^{\mathrm{e}} e^{-\alpha m}, & m \ge 0. \end{cases} \tag{12}$$

The coefficients A^{p}, A^{e}, B^{p}, and B^{e} are determined by the equality of the two expressions in (12) at $m = 0$ and $n = 0, 1$, which yields

$$I^{\mathrm{p}} + A^{\mathrm{p}} = B^{\mathrm{p}}, \quad A^{\mathrm{e}} = B^{\mathrm{e}} \tag{13}$$

and (5) for $m = 0$ and $n = 0, 1$. By eliminating A^{p} and A^{e} by (13), one arrives at a 2×2 system for B^{p} and B^{e}

$$B^{\mathrm{p}}\left[q_n^{\mathrm{p}}(M_n\omega^2 - 4 + 2e^{i\theta}) + q_n^{\mathrm{p}}\right] + B^{\mathrm{e}}\left[q_n^{\mathrm{e}}(M_n\omega^2 - 4 + 2e^{-\alpha}) + q_n^{\mathrm{e}}\right] = -2i\, I^{\mathrm{p}} q_n^{\mathrm{p}} \sin\theta \quad (n = 0, 1). \tag{14}$$

One can calculate the energy conservation relation $|A^{\mathrm{p}}|^2 + |B^{\mathrm{p}}|^2 = |I^{\mathrm{p}}|^2$, and the transmission coefficient is equal to

$$\mathcal{T} = |B^{\mathrm{p}}|^2 / |I^{\mathrm{p}}|^2. \tag{15}$$

Trapped modes. A trapped mode of the lattice with the scatterer at $m = 0$ is a nonzero field u_{mn} in the absence of an incident source field. This means that the system (14) has a nonzero solution for $(B^{\mathrm{p}}, B^{\mathrm{e}})$ with $I^{\mathrm{p}} = 0$. Because $|A^{\mathrm{p}}|^2 + |B^{\mathrm{p}}|^2 = |I^{\mathrm{p}}|^2$, we have $B^{\mathrm{p}} = A^{\mathrm{p}} = 0$, and the field is necessarily exponentially decaying as $m \to \pm\infty$, that is

$$u_{mn} = B^{\mathrm{e}} q_n^{\mathrm{e}} e^{-\alpha|m|} \quad \text{(trapped mode)}.$$

Thus, the condition for a guided mode is the vanishing of the coefficients of B^{e} in (14) for $n = 0, 1$

$$q_0^{\mathrm{e}}(M_0\omega^2 - 4 + 2e^{-\alpha}) + q_1^{\mathrm{e}} = 0, \qquad q_1^{\mathrm{e}}(M_1\omega^2 - 4 + 2e^{-\alpha}) + q_0^{\mathrm{e}} = 0.$$

For given masses M_0 and M_1, we now solve for η and ω, obtaining an isolated pair (η_0, ω_0) that corresponds to a trapped mode. As M_0 and M_1 are varied, the value η_0 that admits a trapped-mode frequency ω_0 changes. (This is analogous to the change of the Bloch wavenumber κ_0 of the guided mode for the dielectric slab when one perturbs the structure.) The eigenfrequency ω_0 is embedded

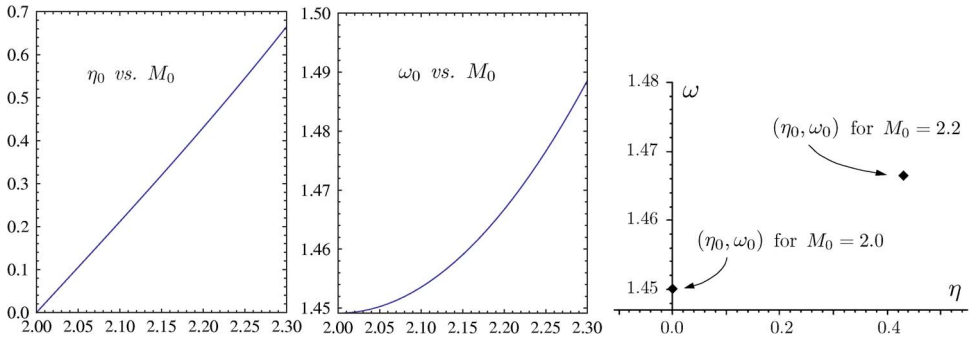

Fig. 3. First two graphs give the values of the asymmetry η_0 in the ambient lattice and the frequency ω_0 corresponding to a trapped mode, as functions of the mass M_0, subject to $M_0 + M_1 = 4$. The frequency interval shown in the second graph is within the spectral band for all the values of η shown in the first graph; thus, all of the trapped mode frequencies are embedded in the continuum. The third graph emphasizes that for each M_0, there is an isolated point (η_0, ω_0) in (η, ω)-space for which the discrete system supports a trapped mode. Resonance occurs when η is perturbed from η_0. The significance of these graphs is explicated in the subsection on "transmission anomalies" in Section 2.

in the continuous spectrum for the lattice system. Using the relation $q_0^e/q_1^e = \eta - \sqrt{1+\eta^2}$, the explicit solution for the masses in terms of η_0 and ω_0 is

$$M_0 = \frac{1}{\omega_0^2}\left[4 - 2e^{-\alpha_0} + \sqrt{1+\eta^2} + \eta_0\right], \qquad M_1 = \frac{1}{\omega_0^2}\left[4 - 2e^{-\alpha_0} + \sqrt{1+\eta^2} - \eta_0\right] \tag{16}$$

in which α_0 is α with (η, ω) replaced by (η_0, ω_0). This leads to the simple relation

$$M_0 - M_1 = \frac{2\eta_0}{\omega_0^2}.$$

This shows that symmetric structures $M_0 = M_1$ admit a trapped mode when $\eta_0 = 0$, that is, when the tensions of the ambient lattice are also symmetric. When $M_0 = M_1 = 2$, the frequency of the trapped mode is $\omega = \sqrt{21/10}$:

$$(M_0, M_1) = (2, 2) \leftrightarrow (\eta_0, \omega_0) = (0, \sqrt{21/10}).$$

This frequency is indicated in Fig. 2.

Transmission anomalies. Let us consider a one-parameter family of scatterers by fixing

$$M_0 + M_1 = 4$$

so that the scatterer is determined by one number M_0 and that the difference $M_0 - 2$ measures its asymmetry. Given M_0, the trapped-mode parameters (η_0, ω_0) are then determined implicitly by (16); their graphs are shown in Fig. 3. The asymmetry of the scatterer $(M_0 \neq 2)$ coincides with the nonvanishing of η_0.

More specifically, the graphs in Fig. 3 should be interpreted as follows. Fixing a value of M_0 specifies a scatterer. Then for this scatterer, these graphs identify an *isolated* pair (η_0, ω_0) in (η, ω)-space for which the system supports a trapped mode. The value of ω_0 is always within the lower part of the spectral band for which the lattice characterized by η_0 supports one propagating and one evanescent harmonic (shown in Fig. 2 for $\eta = 0$). When η is perturbed from η_0, the system for this fixed M_0 and the new η no longer supports a guided mode at any frequency near ω_0.

This destruction of a guided mode due to a perturbation of η is the cause of resonant scattering fields and, hence, transmission anomalies near the frequency ω_0. More specifically, for small enough perturbation of η from η_0, a small interval about ω_0 remains in the spectral band but no

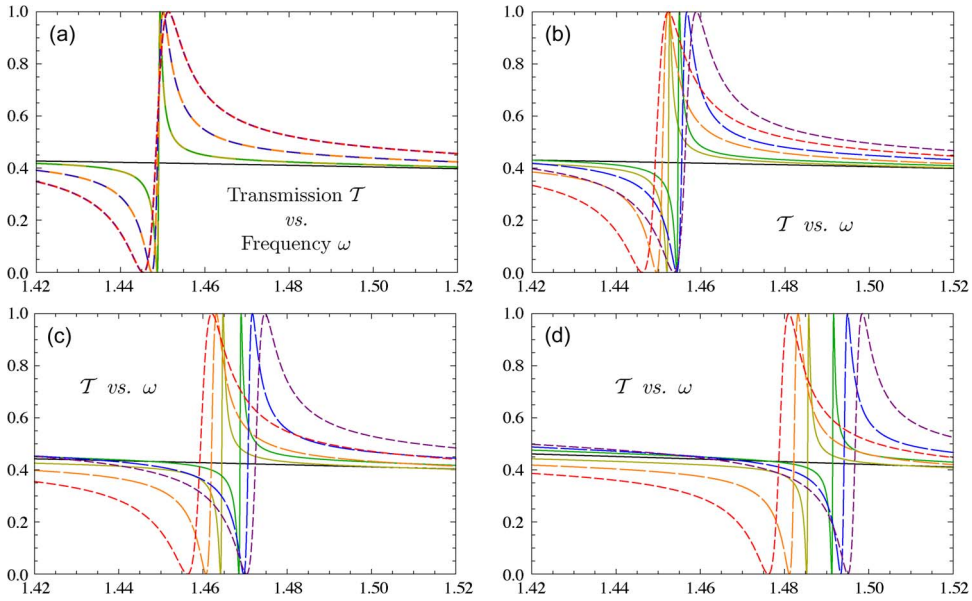

Fig. 4. Resonant anomalies in the transmitted energy $\mathcal{T}$ (15) near trapped mode parameters (η_0, ω_0) of the discrete model, as functions of ω, for various values of the asymmetry η in the ambient lattice and M_0 in the scatterer, subject to $M_0 + M_1 = 4$. The parameters (η_0, ω_0) of the trapped mode depend on M_0 according to the graphs in Fig. 3. In each panel, $\tilde{\eta} = \eta - \eta_0$ assumes the values 0 (no spike, black), ∓ 0.1 (solid line, yellow/green), ∓ 0.2 (long-dashed, orange/blue), ∓ 0.3 (short-dashed, red/violet). (a) $M_0 = 2.0$, $(\eta_0, \omega_0) = (0, 1.449)$; (b) $M_0 = 2.1$, $(\eta_0, \omega_0) = (0.211, 1.453)$; (c) $M_0 = 2.2$, $(\eta_0, \omega_0) = (0.430, 1.467)$; (d) $M_0 = 2.3$, $(\eta_0, \omega_0) = (0.665, 1.488)$.

longer contains an eigenvalue of a bound state. In this interval, scattering fields exhibit high resonant amplitude enhancement and are associated with what are variably called guided resonances [2], or leaky, quasi-guided [13], or resonant modes. Thus the anomalous transmission that we investigate here is due to the annihilation of a nonrobust bound state that turns into resonance within the spectral band of the system and not to the movement of a resonant state into or out of the band.

For a fixed choice of M_0, the transmission coefficient $\mathcal{T}$ exhibits anomalous behavior at values of (η, ω) near the trapped-mode pair (η_0, ω_0), as seen in Fig. 4. In the symmetric case, $M_0 = M_1 = 2$, the anomaly as a function of ω *remains centered about* ω_0 for values of η near $\eta_0 = 0$. In the asymmetric case, the trapped mode occurs at $\eta_0 \neq 0$, and as η is perturbed from η_0, the center of the anomaly *shifts away from* ω_0. The detuned resonant frequency ω_* can be well approximated by a quadratic function of small $\tilde{\eta} = \eta - \eta_0$:

$$\omega_* = \omega_0 + \ell_1 \tilde{\eta} + \frac{1}{2}(r_2 + t_2)\tilde{\eta}^2.$$

The significance of the coefficients will be made clear in the next section.

For a periodic slab, η is replaced by a wavenumber κ parallel to the slab and $M_0 - 2$ is replaced by a structural parameter p. The slab system should operate in a regime of a single propagating diffraction order. Near $(p, \kappa_0) = (0, 0)$, the first graph in Fig. 3 would be like $\kappa_0 \propto \sqrt{p}$, rather than linear as in the discrete system, because guided modes must come in $\pm\kappa_0$ pairs.

3. Universal Formulae

The transmission anomalies exhibited by our discrete system as well as the air/slab system are described by the formula derived in [8] and [11] for scattering by continuous or discrete periodic slabs or waveguides in contact with an ambient medium. In this discussion, we use the notation

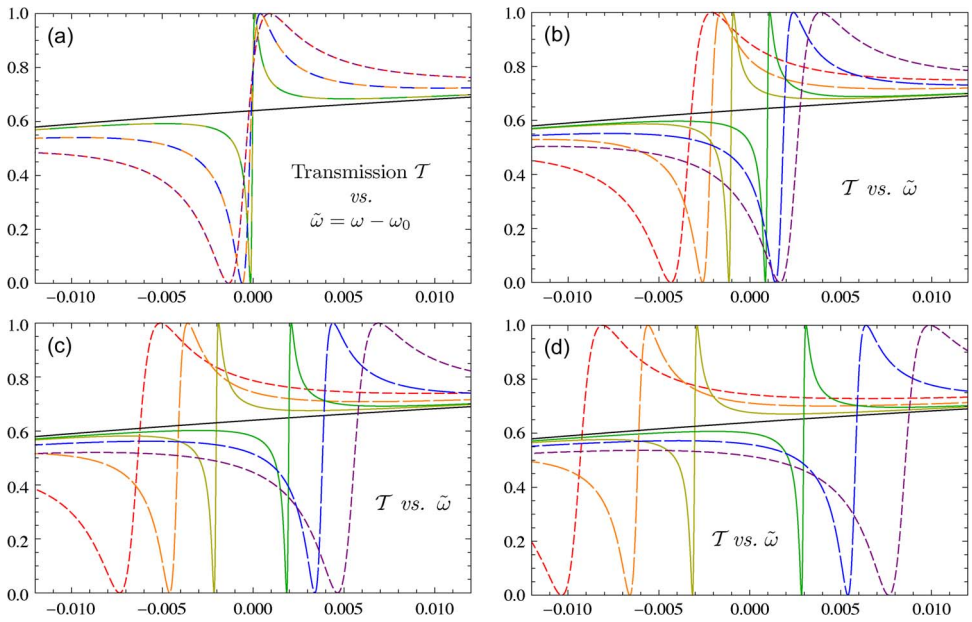

Fig. 5. Analytic formula (17) for transmission anomalies. $\mathcal{T}$ is plotted against $\tilde{\omega} = \omega - \omega_0$ for various values of $\tilde{\eta} = \tilde{\eta} - \tilde{\eta}_0$ and ℓ_1, where an embedded bound state occurs at (κ_0, ω_0). The parameter ℓ_1 controls how the detuning of the resonant anomaly depends on $\tilde{\eta}$ [see (20)]. In each panel, $t_0 = 0.6$, $t_2 = -1.5$, $r_2 = 1.0$, $\zeta = 10$, and $\tilde{\eta}$ assumes the values 0 (no spike, black); ∓ 0.01 (solid line, yellow/green); ∓ 0.02 (long-dashed, orange/blue); ∓ 0.03 (short-dashed, red/violet). (a) $\ell_1 = 0$ (symmetric in $\tilde{\eta}$); (b) $\ell_1 = -0.1$; (c) $\ell_1 = -0.2$; (d) $\ell_1 = -0.3$.

of the discrete system, remembering that η is analogous to a Bloch wavenumber κ along the dielectric slab.

The formula gives the general form of the transmission anomaly for (η, ω) close to (η_0, ω_0):

$$\mathcal{T}(\eta, \omega) = \frac{1}{1 + D^2} + \mathcal{O}\big(|\tilde{\eta}| + \tilde{\omega}^2\big), \qquad D = \frac{r_0|\tilde{\omega} + \ell_1\tilde{\eta} + r_2\tilde{\eta}^2|}{t_0|\tilde{\omega} + \ell_1\tilde{\eta} + t_2\tilde{\eta}^2|}(1 + \zeta\tilde{\omega}) \tag{17}$$

in which $\tilde{\omega} = \omega - \omega_0$, and $\tilde{\eta} = \eta - \eta_0$. A proof of the error estimate is given in [9]. Fig. 5 shows the approximation $1/(1 + D^2)$ for different values of the real number ℓ_1

$$\mathcal{T}(\eta, \omega) \approx \frac{t_0^2|\tilde{\omega} + \ell_1\tilde{\eta} + t_2\tilde{\eta}^2|^2}{t_0^2|\tilde{\omega} + \ell_1\tilde{\eta} + t_2\tilde{\eta}^2|^2 + r_0^2|\tilde{\omega} + \ell_1\tilde{\eta} + r_2\tilde{\eta}^2|^2(1 + \zeta\tilde{\omega})^2}. \tag{18}$$

The formula is rigorous and very general; its derivation relies on a small number of conditions that are satisfied for a large class of lossless linear scattering problems, whether classical or quantum or whether continuous or discrete. It is based on perturbation analysis of a simple branch of the complex relation

$$\omega = W(\eta) = \omega_0 + \ell_1\tilde{\eta} + \ell_2\tilde{\eta}^2 + \cdots \tag{19}$$

defining the locus of generalized trapped modes, which correspond to true trapped modes when η and ω are both real and are associated with leaky modes when either one of them is not real. (For a dielectric slab, one makes the substitution $\eta \mapsto \kappa$, and $\omega = W(\kappa)$ is the dispersion relation for generalized guided modes.) The conditions on which the formula rely are

1) $\omega_0 = W(\eta_0)$ for an isolated point (η_0, ω_0) in the real (η, ω)-plane;
2) conservation of energy;
3) for real η, $\mathrm{Im}(\eta) \leq 0$.

The first condition holds generically for (η, ω) regimes in which the uniform lattice supports one propagating and one evanescent harmonic. The third amounts to the fact that the poles of the scattering matrix are located in the lower half of the complex plane and implies that ℓ_1 is real and Im $\ell_2 \leq 0$.

In (17), r_0 and t_0 are real and positive and satisfy $r_0^2 + t_0^2 = 1$. They are equal to the relative reflected and transmitted energies at $(\tilde{\eta}, \tilde{\omega}) = (0, 0)$. Given that ℓ_1, r_2, and t_2 are real valued, which is the case for our discrete model and the dielectric slab in [11], the relation $\tilde{\omega} + \ell_1\tilde{\eta} + r_2\tilde{\eta}^2 = 0$ describes, up to quadratic order in $\tilde{\eta}$, the locus of 100% transmission, which coincides with the peaks in the transmission graphs. The relation $\tilde{\omega} + \ell_1\tilde{\eta} + t_2\tilde{\eta}^2 = 0$ describes the locus of 0% transmission, which corresponds to the dips of the transmission graphs. The number ℓ_1, which is the linear coefficient of both of these relations as well as the relation (19), is responsible for shifting the anomaly away from ω_0 as η deviates from η_0. The positions of the peak and dip differ only by the quadratic expression $(r_2 - t_2)\tilde{\eta}^2$; thus, *the width of the anomaly is quadratic in* $\tilde{\eta}$. The center of the anomaly can be defined (up to quadratic order in $\tilde{\eta}$) by the detuned resonant frequency

$$\omega_* = \omega_0 + \ell_1\tilde{\eta} + \frac{1}{2}(r_2 + t_2)\tilde{\eta}^2. \tag{20}$$

The number ζ controls the slope of the transmission for $\tilde{\eta} = 0$, which is the overall slope of the graph across the resonances.

The utility of (17) is that one needs only to determine a small number of coefficients in order to obtain a formula that is accurate to $\mathcal{O}(|\tilde{\eta}| + \tilde{\omega}^2)$. It is possible to increase the accuracy by including higher order terms in η in the factors in absolute values in D and higher order terms in both η and ω in the term $(1 + \zeta\tilde{\omega})$.

For a symmetric structure, for which $\eta_0 = 0$, we have $\ell_1 = 0$. This is because, by the change $\eta \mapsto -\eta$ and switching of the indices $n = 0$ and $n = 1$ in the field, one obtains another admissible field with the same transmission coefficient, and thus, $\mathcal{T}$ is symmetric in $\tilde{\eta}$. In this case, there is no linear detuning of the resonant frequency. When the symmetry of the structure is broken, the symmetry of the fields is also broken, and this results in a transmission coefficient that is generally asymmetric in $\tilde{\eta}$ and has $\ell_1 \neq 0$. This asymmetry is manifest in a detuning of the resonant frequency from ω_0 to ω_* that is linear $\tilde{\eta}$. In general, all the parameters r_0, t_0, ℓ_1, r_2, t_2, and ζ will depend on the structure, but it is ℓ_1 that is associated with asymmetry. The role of ℓ_1 is illustrated in Fig. 5, in which all of these parameters are kept fixed except ℓ_1. The bound-state pair (η_0, ω_0) also depends on the structure. The shifting of ω_0 can be seen by comparing the graphs for different structures in Fig. 4; in Fig. 5, the graphs are centered at $\tilde{\omega} = \omega - \omega_0 = 0$.

Relation to the Fano resonance. The formula (17) simplifies to the Fano resonance (1) with $e = (\omega - \omega_0)/(\Gamma/2)$ under the following conditions.

1) $\ell_1 = 0$ (no linear detuning of the resonance),
2) t_2 and r_2 are real (the anomaly attains 0% and 100% transmission),
3) Re$\ell_2 = 0$ (the dispersion relation is purely imaginary to order $\tilde{\eta}^2$),
4) $\zeta = 0$ (the "background" transmission is flat).

The width of the resonance depends quadratically on $\tilde{\eta}$

$$\Gamma = 2\tilde{\eta}^2\frac{t_0|t_2|}{r_0} = 2\tilde{\eta}^2\frac{r_0|r_2|}{t_0} = 2\tilde{\eta}^2\mathrm{Im}\ell_2, \qquad q = \mathrm{sgn}(t_2)\frac{r_0}{t_0}. \tag{21}$$

The complex number ℓ_2 is the coefficient of the quadratic term in the relation $\omega = \omega_0 + \ell_1\tilde{\eta} + \ell_2\tilde{\eta}^2 + \cdots$ (19). Thus, (21) is a form of the Fermi golden rule, relating the imaginary part of the complex frequency of a leaky mode to the width of the anomaly.

4. Nonlinear Scatterer

The effects of Kerr nonlinearity on resonance in dielectric slabs [24], [25], as well as waveguides [26], [27], is important for applications exploiting tunable bistability. In our discrete model, Kerr nonlinearity is introduced into the scatterer by including a fourth-power self-interaction term $\lambda|U_{0n}|^4$

in the Hamiltonian (2). In the Anderson model, an analogous term leads to bistable resonant transmission, which emerges near the bound-state frequency of the linear system and depends on the intensity I of the incident field and the strength λ of the nonlinearity [28]. There, the steady states at a given frequency are determined by the real roots of a cubic polynomial with coefficients depending on I and λ. For the model presented in the present paper, it turns out that the steady states are determined by the simultaneous real roots of four cubic equations in four real variables. Numerical calculations have shown up to five independent states at the same frequency that exhibit resonant behavior for small I or λ not only near but *extending to a continuum of frequencies far above (but not below) the single guided mode frequency* (see Fig. 6).

Similar investigations have been carried out by McGurn *et al.*, [29]–[31] for transmission through nonlinear barriers in photonic crystal waveguides, using a discrete model consisting of 1-D difference equations. Extreme values of the transmission coefficient, depending on the Kerr parameter, occur at the frequencies that correspond to various types of resonant fields in the barrier. In our model, there are multiple harmonic solutions and resonant amplitude enhancement not only at frequencies near that of the bound state but also at a continuum of frequencies ranging from that of the guided mode up to the upper end of the interval that supports exactly one propagating harmonic. This seems to be connected to the fact that the discrete system has two rows of beads instead of one. Further investigation will be required to discover an explanation of this phenomenon and to inquire whether a nonlinear periodic dielectric slab system also exhibits this sort of behavior.

5. Concluding Discussion

The connection established between the line shape of resonant transmission across a scatterer in our discrete model and asymmetry of the structure and the field offers a means of investigating dynamic control of the central frequency and width of resonances through the perturbation of system parameters.

This connection is embodied in an analytic formula in which a parameter in the ambient space, a parameter associated with structural asymmetry and detuning, and the frequencies of the peak and dip, appear explicitly. For a real system, as a dielectric slab structure, a direct correspondence between the parameters in the formula and those of the structure would be established through numerical computations or laboratory experiments. Even so, it is desirable to have a deeper analytic understanding of this correspondence. The discrete model proposed here will facilitate this investigation, as the calculations can be performed by hand, and the model explicitly incorporates a parameter of asymmetry of the scatterer and a parameter analogous to the angle of incidence.

In our model, the peaks and dips of the transmission anomalies reach 100% and 0%. For lossless photonic slab structures, these extremes are commonly observed and, in certain simple cases, can be analytically demonstrated. In a forthcoming communication, we will present a proof that the anomalies attain these extreme values for lossless periodic dielectric slab/air systems that are symmetric about a plane parallel to the slab.

It is worthwhile to compare the mechanism of resonance associated with a guided mode of an open periodic waveguide at a wavenumber–frequency pair (κ_0, ω_0) that is isolated in the (κ, ω) plane to the mechanism associated with the introduction of periodicity into a uniform slab. Fan and Joannopoulos show how small holes periodically placed in an otherwise uniform slab lead to sharp Fano-like transmission and reflection anomalies near the frequencies of certain leaky guided modes or "guided resonances" [2]. As the radius of the holes vanishes, the width of the anomalies tends to zero and the guided resonances tend to true guided modes of the uniform slab (see [2, Fig. 12]). If the period of the slab, which is defined by the placement of the holes, is artificially retained in the uniform slab, the wave vector–frequency relation defining its guided modes can be conceived as a dispersion relation for guided modes at frequencies embedded in the continuum. This is in contrast to the isolated embedded guided mode with which we deal in this paper.

In the case of an isolated embedded guided mode, the wavenumber κ (or, equivalently, the angle of incidence) serves as a perturbation parameter that couples the mode to the extended states,

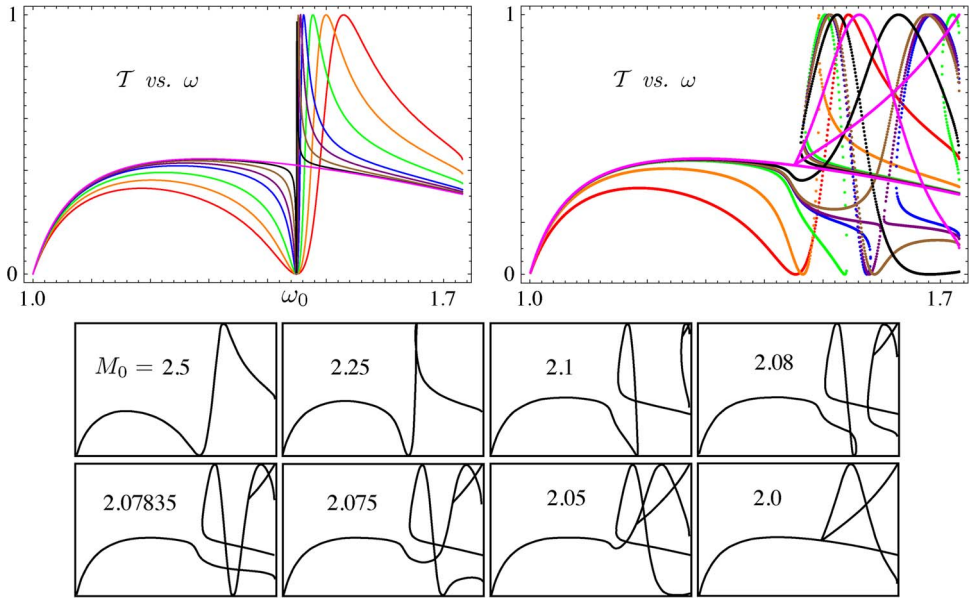

Fig. 6. (**Top right**) Transmission of energy versus frequency for the linear discrete model, which supports a trapped mode at ω_0 with $M_0 = M_1 = 2$ and $\eta = 0$. The transmission is shown for $\eta = 0$ and $M_0 + M_1 = 4$. Each plot corresponds to a fixed value of M_0; as this value ranges from 2.0 to 2.5, a sharp anomaly emerges at ω_0 and becomes wider. (**Top left**) Multivalued transmission graphs for the nonlinear discrete model with $\eta = 0$, $M_0 + M_1 = 4$, $\lambda = 0.01$, and intensity of the incident field $I = 1.0$. Again, M_0 ranges over values from 2.0 to 2.5. The fields corresponding to the upper branch of the transmission graphs exhibit resonant amplitude enhancement in the scatterer. (**Bottom**) Individual nonlinear transmission graphs, from $M_0 = 2.5$ (farthest from resonance) to $M_0 = 2.0$ (structure supporting the trapped mode).

resulting in anomalous scattering. In contrast, the guided mode of a uniform slab is robust under perturbation of κ and, instead, the small radius of the holes serves as the coupling parameter and the mechanism for resonance. The ubiquity of the line shape of the anomaly is discussed in [15], in which the authors generalize a theory developed in [2] for energy transport through a photonic crystal slab mediated by a combination of direct (nonresonant) and indirect (resonance-mediated) channels.

The analysis of [8] and [11], together with the use of discrete models, can be extended to incorporate geometric and material parameters, thus extending (17) and (18) to a much more general class of mechanisms of resonance. In a discrete model, for example, in which plane waves in an ambient 2-D lattice are scattered by a 1-D periodic chain attached to it along a line [32], the formula has been extended to include a parameter of structural coupling between the 1-D and 2-D lattices and has enabled the investigation of a fold bifurcation of resonances. A forthcoming communication will treat the degenerate situation of simultaneous emergence of two Fano-type transmission anomalies from the same bound-state frequency.

References

[1] M. Kanskar, P. Paddon, V. Pacradouni, R. Morin, A. Busch, J. F. Young, S. R. Johnson, J. MacKenzie, and T. Tiedje, "Observation of leaky slab modes in an air-bridged semiconductor waveguide with a two-dimensional photonic lattice," *Appl. Phys. Lett.*, vol. 70, no. 11, pp. 1438–1440, Mar. 1997.

[2] S. Fan and J. D. Joannopoulos, "Analysis of guided resonances in photonic crystal slabs," *Phys. Rev. B, Condens. Matter*, vol. 65, no. 23, p. 235 112, Jun. 2002.

[3] W. Suh, M. F. Yanik, O. Solgaard, and S. Fan, "Displacement-sensitive photonic crystal structures based on guided resonance in photonic crystal slabs," *Appl. Phys. Lett.*, vol. 82, no. 13, pp. 1999–2001, Mar. 2003.

[4] A. E. Miroshnichenko and Y. S. Kivshar, "Engineering Fano resonances in discrete arrays," *Phys. Rev. E, Stat. Phys. Plasmas Fluids Relat. Interdiscip. Top.*, vol. 72, no. 5, p. 056 611, Nov. 2005.

[5] A. Chakrabarti, "Fano resonance in discrete lattice models: Controlling lineshapes with impurities," *Phys. Lett. A*, vol. 366, no. 4/5, pp. 507–512, Jul. 2007.
[6] S. Fan, P. Villeneuve, and J. Joannopoulos, "Rate-equation analysis of output efficiency and modulation rate of photonic-crystal light-emitting diodes," *IEEE J. Quantum Electron.*, vol. 36, no. 10, pp. 1123–1130, Oct. 2000.
[7] J. Song, R. P. Zaccaria, M. B. Yu, and X. W. Sun, "Tunable Fano resonance in photonic crystal slabs," *Opt. Express*, vol. 14, no. 19, pp. 1812–1826, Sep. 2006.
[8] N. Ptitsyna, S. P. Shipman, and S. Venakides, "Fano resonance of waves in periodic slabs," in *Proc. IEEE Int. Conf. Math. Methods EM Theory*, 2008, pp. 73–78.
[9] S. P. Shipman, *Resonant Scattering by Open Periodic Waveguides*, Sharjah, UAE: Bentham, 2009.
[10] G. D. Mahan, *Many-Particle Physics*. New York: Plenum, 1993.
[11] S. P. Shipman and S. Venakides, "Resonant transmission near non-robust periodic slab modes," *Phys. Rev. E, Stat. Phys. Plasmas Fluids Relat. Interdiscip. Top.*, vol. 71, no. 2, pp. 026 611-1–026 611-10, Feb. 2005.
[12] P. Paddon and J. F. Young, "Two-dimensional vector-coupled-mode theory for textured planar waveguides," *Phys. Rev. B, Condens. Matter*, vol. 61, no. 3, pp. 2090–2101, Jan. 2000.
[13] S. G. Tikhodeev, A. L. Yablonskii, E. A. Muljarov, N. A. Gippius, and T. Ishihara, "Quasiguided modes and optical properties of photonic crystal slabs," *Phys. Rev. B, Condens. Matter*, vol. 66, no. 4, pp. 045 102-1–045 102-17, Jul. 2002.
[14] U. Fano, "Effects of configuration interaction on intensities and phase shifts," *Phys. Rev.*, vol. 124, no. 6, pp. 1866–1878, Dec. 1961.
[15] S. Fan, W. Suh, and J. D. Joannopoulos, "Temporal coupled-mode theory for the Fano resonance in optical resonators," *J. Opt. Soc. Amer. A, Opt. Image Sci.*, vol. 20, no. 3, pp. 569–572, Mar. 2003.
[16] W. Suh, O. Solgaard, and S. Fan, "Displacement sensing using evanescent tunneling between guided resonances in photonic crystal slabs," *J. Appl. Phys.*, vol. 98, no. 3, pp. 033 102-1–033 102-4, Aug. 2005.
[17] S. Fan, "Sharp asymmetric line shapes in side-coupled waveguide-cavity systems," *Appl. Phys. Lett.*, vol. 80, no. 6, pp. 908–910, Feb. 2002.
[18] H. Liu and P. Lalanne, "Microscopic theory of the extraordinary optical transmission," *Nature*, vol. 452, no. 7188, pp. 728–731, Apr. 2008.
[19] F. Medina, F. Mesa, and R. Marqués, "Extraordinary transmission through arrays of electrically small holes from a circuit theory perspective," *IEEE Trans. Microw. Theory Tech.*, vol. 56, no. 12, pp. 3108–3120, Dec. 2008.
[20] F. Medina, F. Mesa, and R. Marqués, "Some advances in the circuit modeling of extraordinary optical transmission," *Radioengineering*, vol. 18, no. 2, pp. 103–110, Jun. 2009.
[21] F. Medina, F. Mesa, J. A. Ruiz-Cruz, J. M. Rebollar, and J. R. Montejo-Garai, "Study of extraordinary transmission in a circular waveguide system," *IEEE Trans. Microw. Theory Tech.*, vol. 58, no. 6, pp. 1532–1542, Jun. 2010.
[22] R. Rodríguez-Berral, F. Mesa, and F. Medina, "Circuit model for a periodic array of slits sandwiched between two dielectric slabs," *Appl. Phys. Lett.*, vol. 96, no. 16, pp. 161 104-1–161 104-3, Apr. 2010.
[23] S. Longhi, "Bound states in the continuum in a single-level Fano-Anderson model," *Eur. Phys. J. B*, vol. 57, no. 1, pp. 45–51, May 2007.
[24] V. Lousse and J. P. Vigneron, "Use of Fano resonances for bistable optical transfer through photonic crystal films," *Phys. Rev. B, Condens. Matter*, vol. 69, no. 15, p. 155 106, Apr. 2004.
[25] V. Borulko and D. Sidorov, "Linear and nonlinear resonances in Bragg layered structures with lumped parallel reactive inhomogeneities," in *Proc. IEEE Int. Conf. Math. Methods EM Theory*, 2010, pp. 1–4.
[26] A. R. Cowan and J. F. Young, "Optical bistability involving photonic crystal microcavities and Fano line shapes," *Phys. Rev. E, Stat. Phys. Plasmas Fluids Relat. Interdiscip. Top.*, vol. 68, no. 4, p. 046 606, Oct. 2003.
[27] M. F. Yanik, S. Fan, and M. Soljacic, "High-contrast all-optical bistable switching in photonic crystal microcavities," *Appl. Phys. Lett.*, vol. 83, no. 14, pp. 2739–2741, Oct. 2003.
[28] A. E. Miroshnichenko, S. F. Mingaleev, S. Flach, and Y. S. Kivshar, "Nonlinear Fano resonance and bistable wave transmission," *Phys. Rev. E, Stat. Phys. Plasmas Fluids Relat. Interdiscip. Top.*, vol. 71, no. 3, p. 036 626, Mar. 2005.
[29] A. R. McGurn and G. Birkok, "Transmission anomalies in Kerr media photonic crystal circuits: Intrinsic localized modes," *Phys. Rev. B, Condens. Matter*, vol. 69, no. 23, p. 235 105, Jun. 2004.
[30] A. R. McGurn, "Transmission through nonlinear barriers," *Phys. Rev. B, Condens. Matter*, vol. 77, no. 11, p. 115 105, Mar. 2008.
[31] A. R. McGurn, "Transmission through Kerr media barriers within waveguides and circuits," *Proc. SPIE*, vol. 7395, p. 739 51T, 2009.
[32] N. Ptitsyna, "A discrete model of guided modes and anomalous scattering in periodic structures," Ph.D. dissertation, Louisiana State Univ., Baton Rouge, LA, 2009.